*Original Research*

# Thermal Decomposition Behavior of Polylactic Acid-Based Polyurethane Resin

**Xuefeng Lei[1#], Yiwei Ou[2#], Yuehui Wang[1], Junxian Ma[1]\*, Qiulian Lin[3]**

[1]University of Electronic Science and Technology of China, Zhongshan Institute, Zhongshan 528402, China
[2]School of Light Industry and Chemical Engineering, Guangdong University of Technology, Guangzhou 510006, China
[3]J&D Activated Carbon Filter Co., Ltd. Zhongshan 528402, China

## Abstract

The thermal degradation performance of the polylactic acid (PLA)-based polyurethane resin was investigated by thermogravimetric analysis (TGA), thermogravimetric analysis combined with Fourier transform infrared spectroscopy (TG-FTIR) and thermal cracking gas chromatography/mass spectrometry (PY-GC/MS), while the thermal decomposition mechanism and activation energy were analyzed by different degradation mechanism models. The result demonstrates that the PLA-based polyurethane resin conforms to A2 (nuclear growth) mechanism, and the activation energy of the reaction gradually decreases as the conversion rates increases. The main degradation of polyurethane resin is the decomposition of carbamate, ester group, amide and urea group by comparing the results of the data, and the products of the thermal decomposition are mainly small molecules of primary amine, carbon dioxide, enol, enolic acid and aldehydes.

**Keywords**: polyurethane resin, activation energy, thermal decomposition behavior, degradation mechanism

## Introduction

Traditional petroleum-based polyurethane resins are gradually replaced by bio-based polyurethane resins due to the severe economic and ecological environment [1, 2]. Polylactic acid (PLA)-based polyurethane is a biocompatible and environmentally degradable material which has a wide range of applications in biomedical, flexible packaging and other fields, such as disposable infusion tools, tissue repair materials, artificial skin and food, daily chemical products, and the soft package

[3-5]. Studying the degradation behavior of PLA-based materials has important reference value for promoting its green application, the treatment and control of related industrial wastes, the migration, transformation and elimination mechanisms in the environmental field. At present, research in PLA-based materials mainly be concentrated on the synthesis, application and degradation of PLA-based plastics. An et al. [6] reported a corresponding nanomaterial which was synthesized by graphene oxide with PLA-based polyurethane, the antibacterial experiments indicated that the polyurethane had good biocompatibility and antibacterial properties. While Zhao et al. [5] successfully synthesized PLA-based polyurethane by using polylactic acid polyol. In addition to having balanced mechanical

properties, they observed that it had good damping properties at room temperature; Similarly, Noreen et al. [7] reported a hydroxyethyl cellulose-g-poly (lactic acid) (HEC-g-PLA) blended polyurethane material with antibacterial properties and good biocompatibility, which had good development prospects in biomedicine. In terms of degradation, Jašo [8] fabricated biodegraded polyurethane which was melt blended polylactic acid in different proportions, the test of biodegradation demonstrated that the samples with a co-continuous morphology initially degraded at a higher rate than the rest of the samples due to the higher exposure of the TPU phase in these blends; Dogan et al. [9] evaluated the shape memory and biodegradation behavior of polylactic acid polyurethane, the result indicated that the deformation recovery ability of polyurethane with the polylactic acid was increased, and the degradation rate of bio-enzymes was also accelerated. However, there are few studies on the thermal degradation behavior of PLA-based resins used in adhesives in the field of flexible packaging at present. Besides, based on studying the thermal degradation behavior of polymer materials, exploring the mechanism and principles of thermal degradation of materials and constructing a temperature response model of molecular valence bonds or molecular chain segment breaks during thermal degradation are effective methods to simulate the environmental degradation behavior mechanism and degradation efficiency evaluation of polymer materials by using the characteristics of the principle of polymer time-temperature equivalence.

In this paper, a thermoplastic polyurethane resin with PLA segment was synthesized by hydroxyl-terminated PLA, isocyanate and 1,4-butanediol as the soft, hard segment and binary chain extender respectively. Different kinetic models were used to simulate the thermal degradation process and calculate kinetic parameters, revealing the thermal degradation behavior and mechanism of polylactic acid-based polyurethane resin. To provide theoretical support for the evaluation of environmental degradation behavior and degradation efficiency of degradable polyurethane resin.

## Experimental

### Materials

P(LA-co-CL)-2000 molecular weight polyol was purchased from Shandong Huakai Resin, isophorone diisocyanate (IPDI) and 1,4-butanediol (BDO) were purchased from Macleans Biochemical Technology, Shanghai, dibutyltin dilaurate (DBTDL) from Chemical Reagent Factory, Guangzhou, di-n-butylamine from Lingfeng Chemical Reagent Factory, Shanghai, and isopropanol from Yongda Chemical Reagent Limited Company, Tianjin.

### Preparation of PLA Acid-Based Polyurethane

The polyurethane sample that used in the analysis was synthesized by a two-step method with the co-intercalated polyol of PLA and PCL as the soft segment, the IPDI and chain extender BDO as the hard segment. The preparation of PLA-based polyurethane is shown in Fig. 1.

### Methods of Thermal Degradation Behavior

It is assumed that the thermal decomposition reaction conversion rate and time variation of PLA-based polyurethane follows by Equation (1):
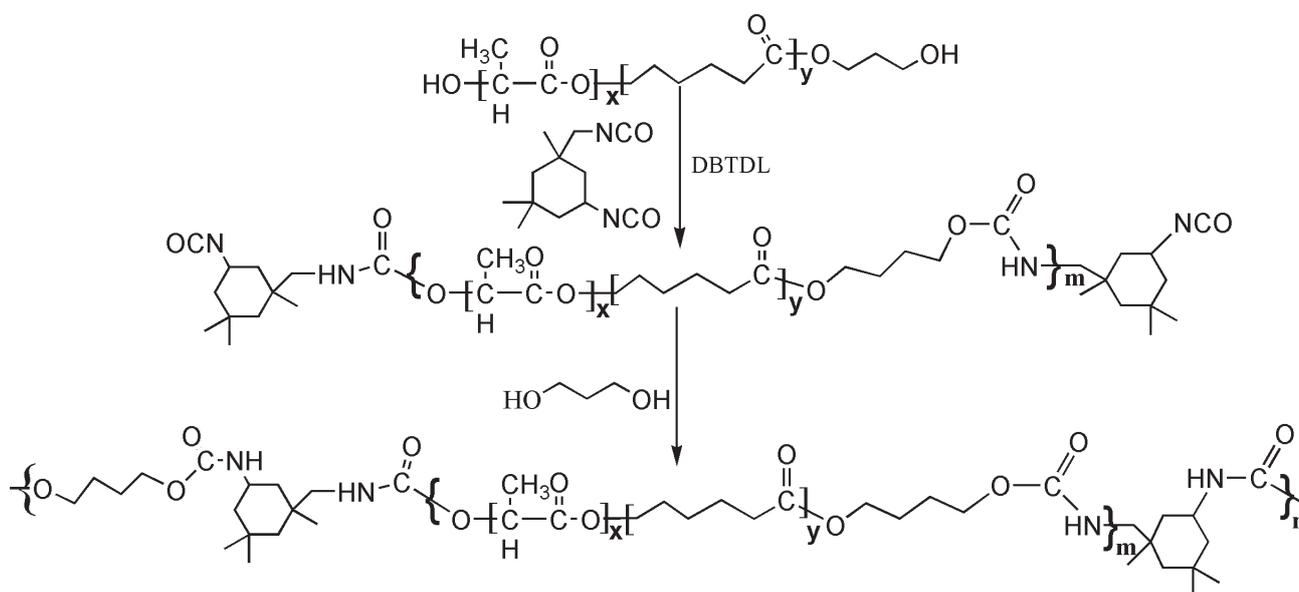


Fig. 1. Preparation of PLA-based polyurethane.

$$\frac{\mathrm{d}\alpha}{\mathrm{d}T} = k(1-\alpha)^n \tag{1}$$

In the formula, $\alpha$ is the conversion rate; $k$ is the reaction rate constant; and $n$ is the reaction order. When the time variation is small enough, the non-isothermal thermal decomposition reaction can be regarded as isothermal. According to the Arrhenius principle [10], the Equation (2) can be obtained as follows:

$$\frac{\mathrm{d}\alpha}{\mathrm{d}T} = \frac{A}{\beta} e^{-\frac{E_a}{RT}} f(\alpha) \tag{2}$$

$T$ is the absolute temperature of pyrolysis; $A$ is the pre-factor; $\beta$ is the heating rate; $E\alpha$ is the activation energy of the thermal decomposition reaction; $R$ is the gas molar constant 8.314 J/(K·mol); $f(\alpha)$ is a reaction mechanism function that depends on the control reaction mechanism. And $\alpha$ can also be named the standardized mass of volatile substances, which can be expressed by the following formula:

$$\alpha = \frac{m_0 - m_t}{m_0 - m_f} \tag{3}$$

Where $m_0$ is the initial mass of the sample, $m_t$ is the mass of the sample at any time t, and $m_f$ is the final mass of the sample after the pyrolysis reaction. Several research models of thermal degradation kinetic behavior are shown as follows.

### Flynn-Wall-Ozawa (FWO) Method

The choice of function mechanism can be avoided by using the Flynn-Wall-Ozawa (FWO) method [11, 12], and the activation energy parameters are calculated under different conversion rate conditions. The equation can be obtained as follows:

$$\log \beta = \log \frac{AE}{Rg(\alpha)} - 2.315 - \frac{0.4567E}{RT} \tag{4}$$

In the formula, $g(\alpha)$ is the integral formula of the thermodynamic expression function. The $\log\beta$ is plotted against $1/T$, and the straight line is obtained by the least square fitting method. The kinetic activation energy can be analyzed according to the slope of the straight line.

### Kissinger-Akahira-Sunose (KAS) Method

The corresponding activation energy parameters under multiple heating rates and different conversion rates also can be calculated by the Kissinger-Akahira-Sunose (KAS) method [13]. The following equation can be obtained:

$$\ln[\frac{\beta}{T^2}] = \ln(\frac{AR}{E}) - \frac{E}{RT} \tag{5}$$

The ln $[\beta/T^2]$ is plotted versus $1/T$, and the corresponding activation energy parameters can be inferred according to the slope.

### Friedman Method

The Friedman method [14] is a differential iso-conversional method, the following equation can be obtained:

$$\ln[\beta(\frac{d\alpha}{dT})] = \ln[Af(\alpha)] - \frac{E}{RT} \tag{6}$$

Where $f(\alpha)$ is a function of $\alpha$, $f(\alpha)$ is a constant when $\alpha$ is constant. The $\ln(\beta(d\alpha/dT)$ is plotted versus $1/T$, and the corresponding activation energy can be calculated.

### Criado Method

The Criado method [15] is often used to judge the thermal decomposition reaction mechanism of polymers, and the following equation can be obtained:

$$\frac{Z(\alpha)}{Z(0.5)} = \frac{[f(\alpha) \cdot g(\alpha)]}{[f(0.5) \cdot g(0.5)]} = (\frac{T_\alpha}{T_{0.5}})^2 \frac{(\frac{d\alpha}{dt})_\alpha}{(\frac{d\alpha}{dt})_{0.5}} \tag{7}$$

In the formula, $T_{0.5}$ and $(d\alpha/dt)_{0.5}$ are the temperature and the corresponding weight loss rate respectively when the conversion rate is $\alpha = 0.5$, $f(\alpha)$ and $g(\alpha)$ are the mechanism functions of the reaction, as shown in Table 1. It is used to distinguish the thermal decomposition mechanism through comparing the consistency between the model curve and the simulated curve on the thermal decomposition process of test sample.

### Coast-Redfern (C-R) Method

Coast-Redfern (C-R) method [15-17] is a common exponential integration method, the following equation can be obtained:

$$\ln[\frac{g(\alpha)}{T^2}] = \ln(\frac{AR}{\beta E}) - \frac{E}{RT} \tag{8}$$

The reaction mechanism function $g(\alpha)$ is substituted into the formula, the $\ln[g(\alpha)/T^2]$ is plotted versus $1/T$, the value of $E$ obtained by different reaction mechanisms can be analyzed by comparing with other methods

to determine the corresponding reaction mechanism. Table 1 presents the algebraic expressions of functions of common solid-state thermal decomposition mechanism of polymer.

## Characterization

### *TGA*

The decomposition process and kinetic parameters of polyurethane was analyzed by the thermogravimetric analyzer (TA instrument from Waters, USA) in a nitrogen atmosphere. The nitrogen flow rate was 25 mL/min. and the thermogravimetric curves were obtained at four different heating rates (5, 10, 15 and 20ºC/min.) from room temperature to 600ºC.

### *TG-IR*

The TG-FTIR instrument is consisted of a thermal gravimeter (TG209, Netzsch Instruments, Germany), a Fourier transform infrared spectrometer (Tensor 27, Bruker Optics Inc., Germany), and a transfer tube with an inner diameter of 1 mm was connected the TG and the infrared cell. The test conditions were as follows: the nitrogen flow was 30 ml/min, the linear heating rate was 20ºC/min., from 40ºC to 800ºC, the resolution and spectral range of the Fourier infrared transform spectrum were 4 $cm^{-1}$ and 4000-400 $cm^{-1}$ respectively, the spectral scan interval was 8 seconds.

### *PY-GC/MS*

The thermal cracking of polyurethane was carried out in the Perkin-Elmer Clarus 680 GC-SQ8MS gas chromatography-mass spectrometer, and the specific cracked products after high temperature were analyzed. The starting temperature was 40ºC, lasted 5 minutes, and then raised the temperature to 280ºC for 3 min. at the rate of 10ºC/min., injected at 280ºC, the carrier gas was nitrogen, the constant temperature flow was 1 ml/min., the split ratio was 10:1, and the cracking was carried out at 500ºC. The chemical family in the library was used to identify the compounds generated by the retention time and the corresponding peak area.

## Results and Discussion

### Thermal Degradation Behavior and Kinetics

The thermogravimetric (TG) and derivative thermogravimetry (DTG) curves of PLA-based polyurethane at different heating rates are illustrated in Fig. 2. The thermal decomposition processes are divided into three stages by means of split-peak fitting according to Gaussian curve. And their characteristic data are determined from the TG, DTG, first time derivatives and second time derivatives curves of DTG at different heating rates. Here using DTG curve at the heating rate of 5ºC/min as an example (Fig. 3), the extrapolated onset decomposition temperature was obtained by extrapolating the slope of the DTG curve

Table 1. Algebraic expression of functions of solid-state polymer thermal decomposition mechanism.

| Reaction mechanism | | $g(\alpha)$ | $f(\alpha)$ |
|---|---|---|---|
| Reaction order mechanism | First order reaction F1 | $-\ln(1-\alpha)$ | $1-\alpha$ |
| | Secondary reaction F2 | $(1-\alpha)^{-1}$ | $(1-\alpha)^2$ |
| | Tertiary reaction F3 | $(1-\alpha)^{-2}$ | $(1-\alpha)^3$ |
| Phase boundary control mechanism | Shrinking cylinder R2 | $1-(1-\alpha)^{1/2}$ | $2(1-\alpha)^{1/2}$ |
| | Shrink sphere R3 | $1-(1-\alpha)^{1/3}$ | $3(1-\alpha)^{2/3}$ |
| Diffusion control mechanism | One-dimensional diffusion D1 | $\alpha^2$ | $(2\alpha)^{-1}$ |
| | Two-dimensional diffusion D2 | $(1-\alpha)\ln(1-\alpha)+\alpha$ | $[-\ln(1-\alpha)]^{-1}$ |
| Nuclear growth mechanism | A2 | $[-\ln(1-\alpha)]^{1/2}$ | $2(1-\alpha)g(\alpha)$ |
| | A3 | $[-\ln(1-\alpha)]^{1/3}$ | $3(1-\alpha)g(\alpha)$ |
| | A4 | $[-\ln(1-\alpha)]^{1/4}$ | $4(1-\alpha)g(\alpha)$ |
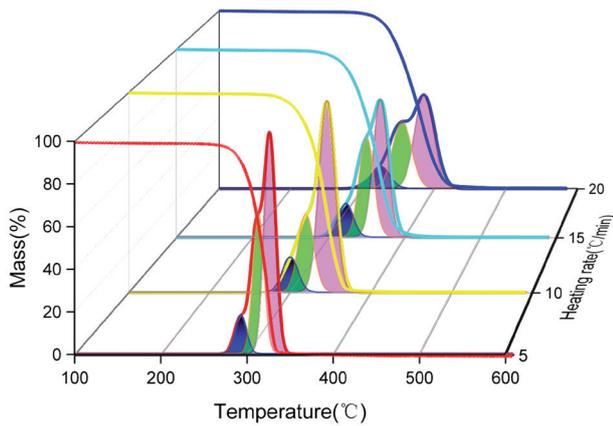
Fig. 2. TG and DTG curve of PLA-based polyurethane at different heating rates.
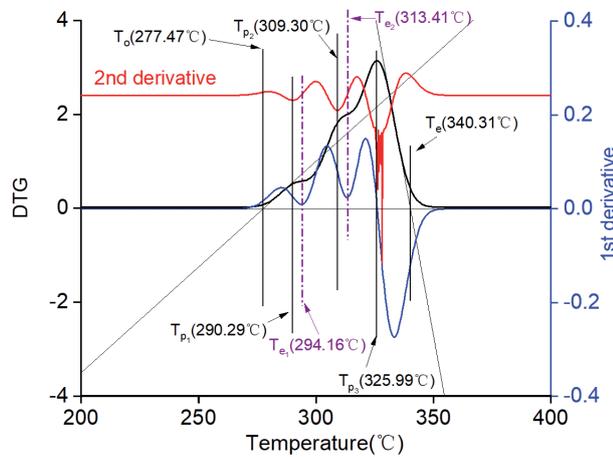


Fig. 3. Determination of decomposition characteristic data of PLA-based polyurethane.

obtained and corresponded to the minimum of the second derivative curve of the DTG curve. The weight loss percentage corresponding to $T_p$ is represented with $WL_p$. The end temperature, $T_e$, is defined by extrapolating the slope of the DTG curve corresponding to the local minimum of the first derivative curve in this region and down to the baseline of the DTG curve. The weight loss percentage corresponding to $T_e$ is marked with $WL_e$. According to above, the decomposition characteristics data of PLA-based polyurethane are presented in Table 2 at different heating rates.

In Figs 2 and 3 and Table 2, when the PLA-based polyurethane is degraded at a heating rate of 20ºC/min., its degradation starts from 294.15ºC and ends at 415.74ºC with a degradation rate of (mass loss rate) 93.57%. The degradation process is divided into three stages: the first stage is from 294.15 to 318.16ºC, with a degradation rate of 2.41%; the second stage is from 318.16 to 358.67ºC, with a degradation rate of 26.38%, and the third stage is from 358.67 to 415.74ºC, with a degradation rate of 66.16%. With the increase of degradation warming rate, the initial and end temperatures of degradation of the specimens increase, the degradation temperature range become larger and the degradation rate decreases; the degradation process still shows three stages, and the peak temperature of the degradation heat absorption peak of each stage move to the high temperature area, and the degradation rate of different stages do not show regular changes, which indicates that the change of warming rate has a complex effect on the degradation behavior of different stages of the degradation process. The reason for this result may be due to the difference in sensitivity to temperature of sample components, heat transfer barrier effect between broken chain segments, and further degradation mechanism of degradation product fragments at different degradation stages with the change of warming rate [19, 20].

In order to better understand the thermal decomposition process of PLA-based polyurethane, the non-isothermal kinetic integration FWO method, KAS method and differential FD method are used to analyze the kinetics of polyurethane and obtain the activation energy of kinetic parameters. The related fitting

in correspondence with the first local maximum in first derivative curve and down to the baseline of the DTG curve [18].

The peak temperature, $T_p$, is determined by DTG peak, where the maximum decomposition rate is

Table 2. Decomposition characteristics data of PLA-based polyurethane at different heating rates.

| $\beta^*$ | Stage 1 | | | | Stage 2 | | | | Stage 3 | | | | $T_e$-$T_o$ | $\Delta WL^*$ |
|---|---|---|---|---|---|---|---|---|---|---|---|---|---|---|
| | $T_o$ | $T_{p1}$ | $T_{e1}$ | $WL_{e1}$ | $T_{o2}$ | $T_{p2}$ | $T_{e2}$ | $WL_{e2}$ | $T_{o3}$ | $T_{p3}$ | $T_e$ | $WL_{e3}$ | | |
| ºC/min. | ºC | | | % | ºC | | | % | ºC | | | % | ºC | % |
| 5 | 277.47 | 290.29 | 294.16 | 4.07 | 294.16 | 309.30 | 313.41 | 27.99 | 313.41 | 325.99 | 340.31 | 63.95 | 62.84 | 96.01 |
| 10 | 281.72 | 293.52 | 298.63 | 4.61 | 298.63 | 315.64 | 321.43 | 23.79 | 321.43 | 345.14 | 366.85 | 65.62 | 85.13 | 95.02 |
| 15 | 290.54 | 309.09 | 315.43 | 3.23 | 315.43 | 341.70 | 348.77 | 27.08 | 348.77 | 367.28 | 391.36 | 64.64 | 100.82 | 94.95 |
| 20 | 294.15 | 311.48 | 318.16 | 2.41 | 318.16 | 348.81 | 358.67 | 26.38 | 358.67 | 387.41 | 415.74 | 66.16 | 121.49 | 93.57 |

* $\beta$: Heating rate; $\Delta WL$: Weight loss of the whole thermal decomposition process from $T_o$ to $T_e$

and calculation results are shown in Table 3 and Figs 4 and 5.

In the first stage (0<α≤0.15), the linear fits based on the FWO and KAS methods, respectively, are almost parallel, which indicates the activation energy of degradation calculated for lactic acid-based polyurethanes at different conversion rates is approximated as a constant, and consequently implies the possibility of single reaction mechanism (or the unification of multiple reaction mechanisms). In the second and third stages, the parallelism of the straight lines fitted according to the above two methods deteriorated, and the slope of the straight lines changed more and more obviously as the conversion rate became larger, and the activation energy gradually decreased accordingly (the results are shown in Fig. 5a), which predicted that the thermal degradation reaction mechanism changed at α>0.15, and there might be autocatalytic effects in the degradation mechanism, leading to more complicated modeling and simulation of the degradation process. The trends of the lines fitted by the FWO and KAS methods show that the thermal degradation of PLA based thermoplastic polyurethane belongs to a possible single reaction mechanism at low conversions (α≤0.15) and to a variable mechanism when higher conversions are reached (α>0.15).

As the goodness of fit (GOF) considered, The $R^2$ values range of fitting linear of FWO method is from 0.9443 to 0.9948 while that of KAS method is between 0.9103 and 0.9907 at different conversion rate (The results are presented in Fig. 5b). The $R^2$ values, reflecting reliability of linear fit, are closer to 1 at moderate conversions (0.15≤α≤0.65) than at low conversions (α<0.15) or high conversions (α>0.65). However, the lines fitted with the differential FD method show non-parallelism at different stages of the whole thermal decomposition process, revealing the non-constant characteristics of activation energy calculated at different conversion rate. Furthermore, there is a large dispersion of the $R^2$ values of the fitted lines, which are far from 1. Therefore, it is not appropriate to use the Friedman method as one of

Table 3. Activation energies of PLA based-polyurethane obtained by FWO, KAS and FD methods at different conversion rates.

| Stages | α | FWO method | | KAS method | | FD method | |
|---|---|---|---|---|---|---|---|
| | | $E$(kJ/mol) | $R^2$ | $E$(kJ/mol) | $R^2$ | $E$(kJ/mol) | $R^2$ |
| First stage | 0.05 | 26.27 | 0.9443 | 22.58 | 0.9153 | 26.57 | 0.9332 |
| | 0.07 | 26.39 | 0.9652 | 22.63 | 0.9458 | 21.50 | 0.7509 |
| | 0.09 | 26.42 | 0.9769 | 22.59 | 0.9633 | 25.81 | 0.9750 |
| | 0.10 | 26.39 | 0.9803 | 22.55 | 0.9684 | 21.01 | 0.8971 |
| | 0.15 | 26.26 | 0.9911 | 22.28 | 0.9851 | 20.71 | 0.6326 |
| Second stage | 0.20 | 26.04 | 0.9935 | 21.99 | 0.9888 | 18.64 | 0.9156 |
| | 0.25 | 25.72 | 0.9947 | 21.59 | 0.9907 | 10.87 | 0.9986 |
| | 0.30 | 25.25 | 0.9948 | 21.03 | 0.9905 | 16.42 | 0.9199 |
| | 0.35 | 24.74 | 0.9946 | 20.44 | 0.9901 | 17.38 | 0.9086 |
| | 0.40 | 24.23 | 0.9941 | 19.85 | 0.9888 | 13.84 | 0.9567 |
| | 0.45 | 23.80 | 0.9937 | 19.35 | 0.9878 | 12.55 | 0.9631 |
| Third stage | 0.50 | 23.34 | 0.9927 | 18.84 | 0.9860 | 12.48 | 0.8544 |
| | 0.55 | 22.94 | 0.9916 | 18.36 | 0.9866 | 11.50 | 0.8027 |
| | 0.60 | 22.57 | 0.9904 | 17.93 | 0.9832 | 10.87 | 0.8636 |
| | 0.65 | 22.22 | 0.9892 | 17.52 | 0.9805 | 10.49 | 0.8461 |
| | 0.70 | 21.89 | 0.9884 | 17.13 | 0.9780 | 9.88 | 0.8478 |
| | 0.75 | 21.53 | 0.9876 | 16.73 | 0.9758 | 8.15 | 0.5752 |
| | 0.80 | 21.10 | 0.9867 | 16.23 | 0.9737 | 6.01 | 0.4518 |
| | 0.85 | 20.56 | 0.9850 | 15.61 | 0.9713 | 9.96 | 0.5580 |
| | 0.90 | 19.88 | 0.9807 | 14.84 | 0.9566 | 2.99 | 0.3263 |
| | 0.95 | 19.09 | 0.9734 | 13.94 | 0.9385 | 4.64 | 0.0111 |
| Average $E^*$ | | 24.28 | | 19.92 | | 14.16 | |

a)



b)



c)
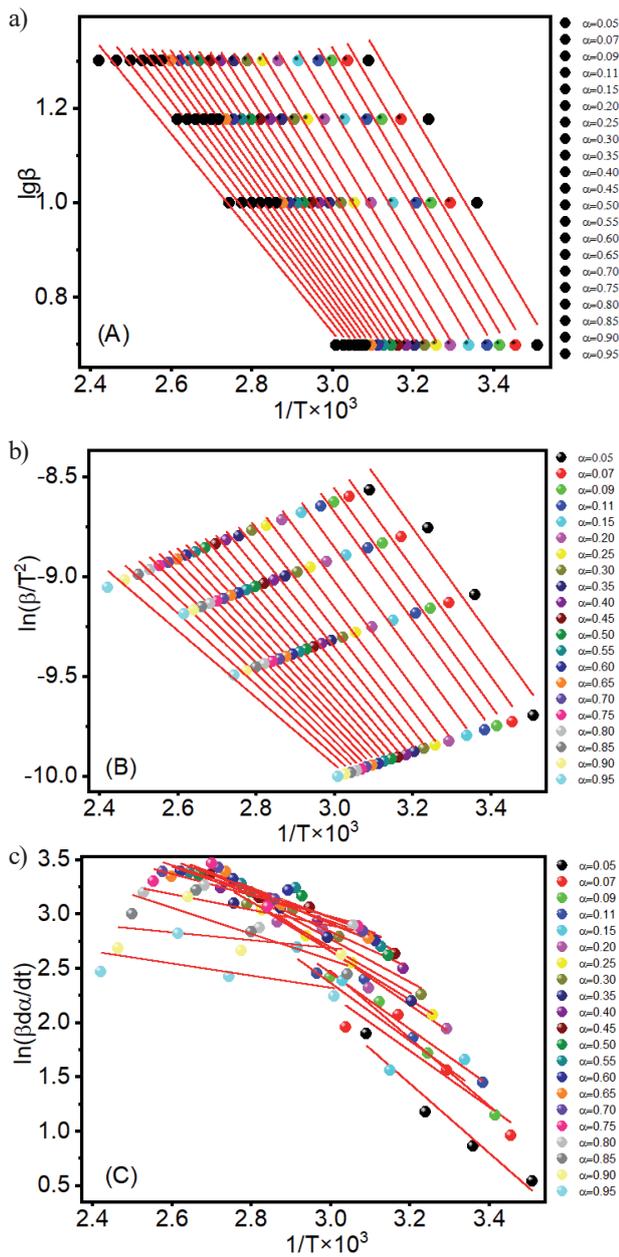


Fig. 4. The fitting curves of PLA based-polyurethane by FWO a), KAS (b) and FD c) methods at different conversion rates.

a)



b)



Fig. 5. Activation energy calculated and fitting reliability vs α according to FWO and KAS methods.

the kinetic models for the thermal decomposition of PLA-based polyurethane.

Considering the above results together, the conversion rates range from 0.15 to 0.65 ($R^2 > 0.98$) is emphasized, rather than the entire decomposition process, which may offer a simplified and more meaningful way to model the thermal decomposition behavior of PLA-based polyurethane. As a result, the average apparent activation energies calculated by FWO and KAS are 24.28 kJ/mol and 19.24 kJ/mol at different conversion rate.

In order to determine the decomposition reaction mechanism of PLA-based polyurethane, the thermal decomposition process was explored according to the Criado reaction mechanism model and the Coast-Redfern

method (C-R method). Based on the different reaction mechanisms g(x) in Table 1 and the experimental thermal decomposition curves of PLA-based polyurethanes at a heating rate β of 10ºC/min, the Z(x)/Z(0.5) master curve can be plotted using Equation (7). Fig. 6 shows the Z(x)/Z(0.5) master and the experimental curves of the PLA-based polyurethane, respectively. It can be seen that the trend of experimental sample curve, is close to the master curves of R2, R3, A2, A3, and A4, and nearly overlaps the master curve (Z(R2)/Z(0.5)) of A2. This result indicates that the thermal decomposition behavior of PLA-based polyurethane complies with A2 reaction mechanism model, and belongs to the nuclear growth mechanism [21]. For further verification, the corresponding reaction mechanism functions were substituted into the C-R method, and the relevant kinetic parameters of the experimental samples were calculated. The results are presented in Fig. 7 and Table 4.

It can be observed that the activation energy (23.11 kJ/mol) calculated by the reaction mechanism function A2 is closest to that obtained by FWO method (24.28kJ/mol). While the activation energies calculated
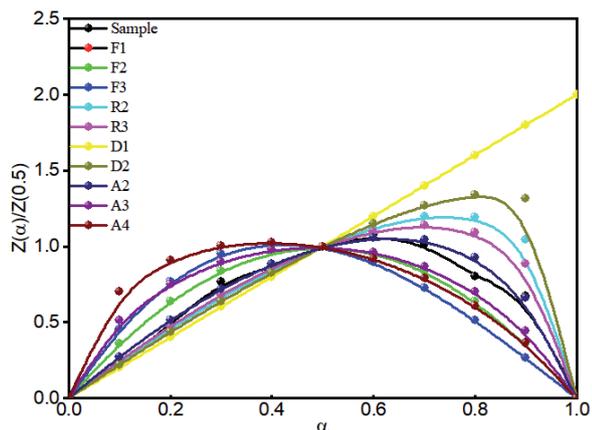
Fig. 6. Master plots of different kinetic models and experimental data at 10 K/min. calculated by Eq. (7) for thermal decomposition of polylactic acid-based polyurethane.
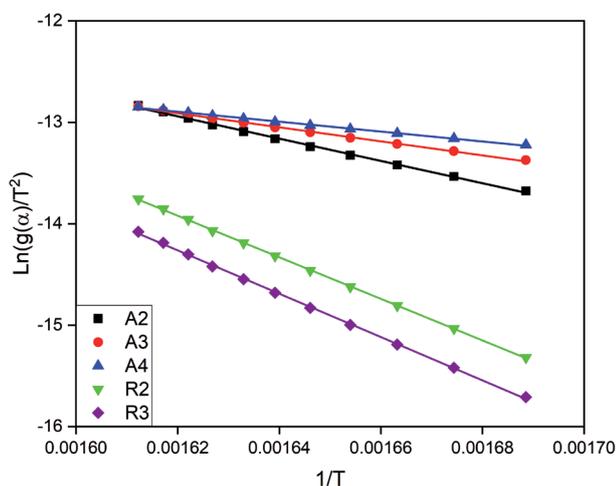


Fig. 7. Linear fitting curves of thermal decomposition of polylactic acid-based polyurethane by Coast-Redfern methods.

Table 4. Activation energies and pre-exponential factors of PLA based-polyurethane obtained by Coast-Redfern methods at different thermal decomposition mechanism models.

| Mechanism | Slope $k$ | $E$/(kJ/mol) | ln$A$ | $R^2$ |
|-----------|-----------|--------------|--------|--------|
| R2 | -5.21 | 43.31 | 6.311 | 0.99703 |
| R3 | -5.53 | 45.97 | 6.979 | 0.99911 |
| A2 | -2.78 | 23.11 | -0.3449 | 0.99838 |
| A3 | -1.63 | 13.55 | -4.1961 | 0.99824 |
| A4 | -1.06 | 8.81 | -6.289 | 0.99808 |

by other mechanism functions are very different from those calculated by the FWO method, indicating that the thermal decomposition mechanism function of PLA-based polyurethane is $g(\alpha) = [-\ln(1-\alpha)]^{1/2}$, which is consistent with the nuclear growth mechanism.
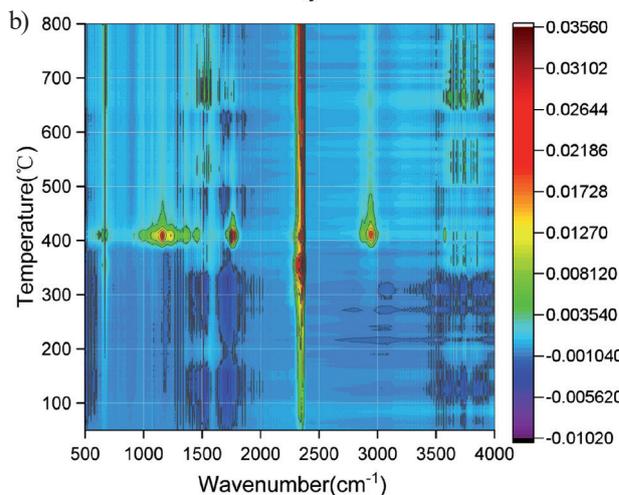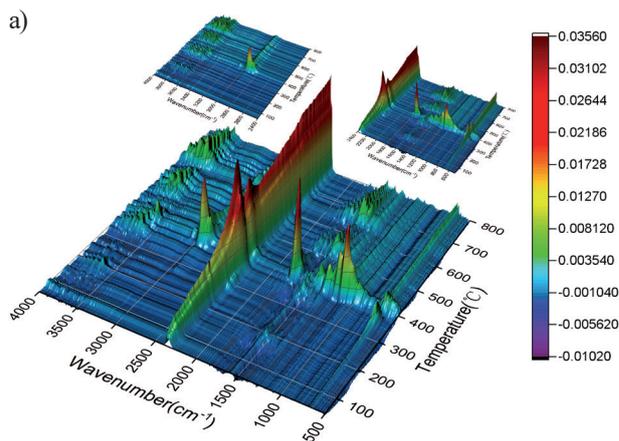


Fig. 8. IR spectra of decomposition products of PLA-based polyurethane under different temperatures at a heating rate β of 10ºC/min.: Full view a) and projection b).

## TG-FTIR Analysis

TG-IR result of PLA-based polyurethane is shown in Fig. 8.

Absorption peaks located at 1154 cm⁻¹, 1234 cm⁻¹, 1350 cm⁻¹, 1454 cm⁻¹, 1569 cm⁻¹, 1755 cm⁻¹, 2275cm⁻¹, 2340 and 668 cm⁻¹, 2937 and 2968 cm⁻¹, 3500 to 3700 cm⁻¹ are found in the IR spectra of the thermal decomposition products collected at different temperatures, respectively represent the characteristic functional groups of −C−O− (alcohol group), −C−O− (carboxyl group), −C−N, −CH₃, −NH−, −C(=O)−, −NCO, $CO_2$, −CH₃ and −CH₂−, −OH or −NH−. In the range of 150–250ºC, the absorption peaks representing −NH− at 1569 cm⁻¹, −NCO at 2275 cm⁻¹, $CO_2$ at 2340 cm⁻¹ and −OH at 3500–3700 cm⁻¹ appear weaker. The result indicates that the thermoplastic PLA-based polyurethane contains a small amount hydrones and free isocyanates, which react with each other to produce $CO_2$. With the increase of decomposition temperature, the −C−O− group at 1154 cm⁻¹, −C−NH−group at 1350 and 1569 cm⁻¹, −C(=O)−OH− group at 1755, 1234 and 3500-3700 cm⁻¹, and −CH₃ and −CH₂ groups at 1454, 2968 and 2937 cm⁻¹ show an increase and then decrease in the intensity of

the absorption peaks between 350-450ºC; the intensity of $CO_2$ peaks located at 2340 and 668 cm$^{-1}$ show two increases and then decreases between 300-380ºC and 380-450ºC, respectively, and the peak temperatures are located at 350 and 410ºC, respectively, the reason for this result is that the ester groups in the soft segments of urethane and PLA-based polyurethane break at different temperature stages to form $CO_2$, respectivThis result indicates that the temperature range of 350-450ºC is the main stage for the breakage of PLA-based polyurethane chain segments, where the breakage of carbamate and ester groups occurred successively, forming a large amount of $CO_2$, carboxyl carbon chains, amino carbon chains and hydrocarbon carbon chains. While further breakage of these chain segments leads to weakening of the intensity of the corresponding absorption peaks. When the decomposition temperature is between 500 and 800ºC, only the absorption peaks representing –
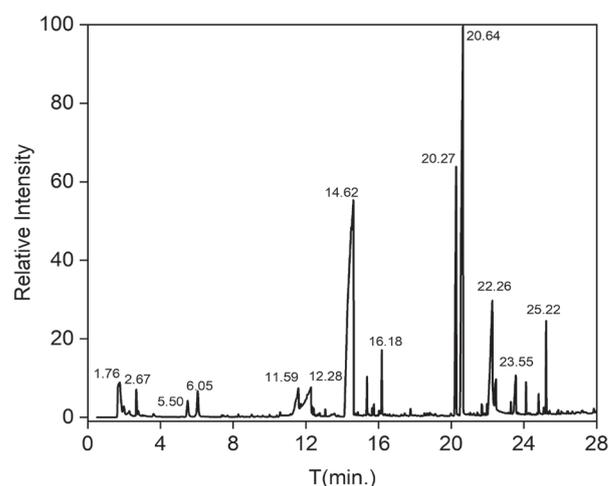


Fig. 9. The chromatogram of polylactic acid-based polyurethane at 500ºC.

Table 5. Products of polylactic acid-based polyurethane at different retention.

| Retention time/min. | Structural formula | Molecular formula | Peak area/% |
|---|---|---|---|
| 1.76 | O=C=O | $CO_2$ | 3.57 |
| 2.67 | | $C_4H_6O$ | 1.10 |
| 5.50 | | $C_6H_8O_2$ | 0.83 |
| 6.05 | | $C_6H_{12}$ | 1.28 |
| 11.59 | HO—OH | $C_4H_{10}O_2$ | 2.39 |
| 12.28 | | $C_6H_{10}O_2$ | 3.60 |
| 14.62 | | $C_6H_{12}$ | 35.70 |
| 15.36 | | $C_8H_{14}O_2$ | 0.70 |
| 16.18 | | $C_8H_{14}O_2$ | 1.06 |
| 20.27 | | $C_{12}H_{18}N_2O_2$ | 8.03 |
| 20.64 | | $C_{10}H_{18}O$ | 21.47 |
| 22.26 | | $C_7H_{12}O_4$ | 8.57 |
| 23.55 | | $C_{10}H_{21}NO$ | 1.62 |
| 25.22 | | $C_{13}H_{24}O_2$ | 1.47 |

NH–, –CH$_3$ and –CH$_2$–, –OH groups and CO$_2$ appear, but the peak intensity become significantly weaker; the absorption peak of representing –C(=O)–OH groups is basically absent, which indicates that when the decomposition temperature is greater than 500ºC, the main thermal decomposition behavior occurred is the further decomposition of the broken fragments into small molecules of hydrocarbons, alcohols and amines, while the carboxylic acid-based chain segments are converted to CO$_2$.

## PY-GC/MS

The cleavage at high temperature can be used to investigate the scission laws of the chemical bonds on main chain of the PLA-based polyurethane [22, 23]. According to the results of PY-GC/MS and the chemical structure of polyurethane, the pyrolysis products of PLA-based polyurethane at 500ºC are inferred and listed in Fig. 9 and Table 5. Demonstratively the thermal decomposition of polylactic-based polyurethane mainly generates carbon dioxide, isocyanate, amine, alcohol, olefin and a small amount low molecular ester through the fracture of chemical bonds at different positions. Correspondingly it consists of three pathways for the chemical bond-fracturing of polylactic-based polyurethane according to the results of Fig. 9 and Table 5. Firstly, the urethane segments are cracked into isocyanates and polyester polyols through the fracture of carbon-oxygen bonds on the right side of the ether bond in the ester groups. Furthermore, the isocyanates

are broken into primary amines, carbon dioxide and so on. The polyester polyols are disassociated to carboxylic acids and fatty alcohols, which generates olefins or cyclic ether by dehydrating carbon dioxide or hydrone at high temperature. Secondly the carbamates are ruptured into carbamic acids and unsaturated polyester by the breaking of carbon-oxygen bonds on the left side of the ether bond in the ester groups. The carbamic acids are broken into primary amines and carbon dioxide while the unsaturated polyester is splitted into aldehydes or olefins [24, 25]. Thirdly, the carbamate chains are directly converted into amines and carboxylate esters containing aliphatic rings by carbon dioxide removing from carbamate structures.

## Decomposition Mechanism

The thermal degradation mechanism of PLA-based polyurethane materials can be divided into three stages according to the results of TG-IR and PY-GC-MS. The first stage is mainly represented of volatilizing of hydrones and unreacted isocyanates, which react with each other to generate carbon dioxide in the temperature range of 150-250ºC. The second stage is located at 300-450ºC, which is the main temperature region for carbamate chain segment bond breakage. Here the chemical bond in the NH–C(=O)–O– structures break at different positions, forming carbon dioxides, hydroxyl segments, carboxyl segments, isocyanates and amino segments. Furthermore, the ester group structures in the co-polyester with PLA and PCL crack into carbon
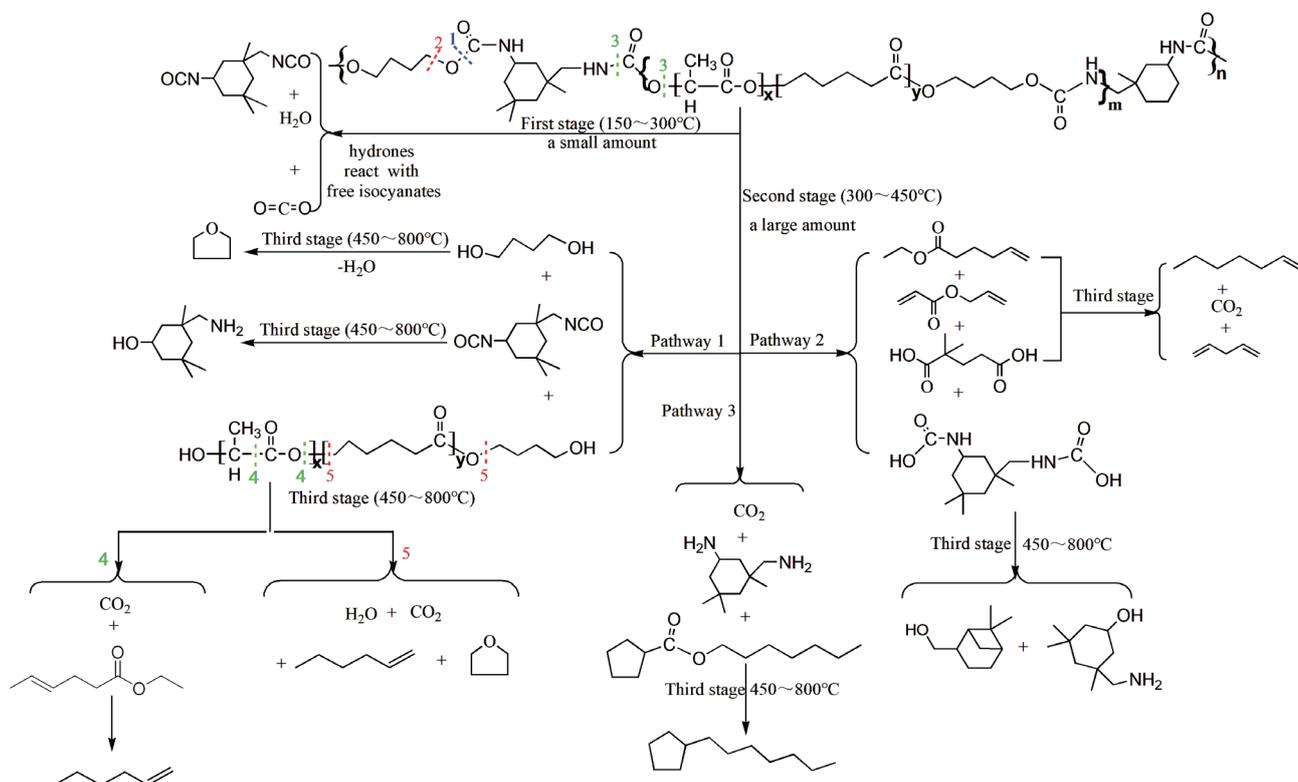


Fig. 10. The breaking mechanism of the main bond in polylactic acid-based polyurethane.

dioxides, hydrocarbon molecules, acids, alcohols, etc. The third stage is above 450ºC, taking on further cracking of the fracture products and forming to small molecular alcohols, hydrocarbons, carbon dioxides and so on. The decomposition mechanism of polylactic acid-based polyurethane is deduced into Fig. 10.

## Conclusions

In this paper, the thermal degrade behavior of PLA-based polyurethane materials is characterized by TGA, TG-IR and PY-GC-MS, including thermal stability, dynamic parameters and dynamic model, decomposition products and degradation mechanism. The degradation process of PLA-based polyurethane materials begins from 281.72ºC, determined by the double tangent method, to 366.85ºC and weight loss percentage reaches to 95.02% at a linear heating rate of 10ºC/min. The dynamic activation energy simulated and calculated according to FWO, KAS and FD, is respectively 24.28 kJ/mol and 19.92 kJ/mol, except the result by FD method for its poor correlation. And the results of CR method and Criado method show that the thermal degradation mechanism model of PLA-based polyurethane conforms to the function. The thermal degradation mechanism of PLA-based polyurethane materials can be divided into three stages according to the results of TG-IR and PY-GC-MS, and the detailed process of main bond breaking at each stage is also speculated.

## Acknowledgments

## Conflict of Interest

The authors declare no conflict of interest.

## References

1.  MOHANTY, A.K., MISRA M., DRZALL L.T. Sustainable bio-composites from renewable resources: opportunities and challenges in the green materials world. Journal of Polymers and the Environment, **10** (1/2), 19, **2002**.
2.  ZHU, Y., ROMAIN C., WILLIAMS C.K. Sustainable polymers from renewable resources. Nature, **540** (7633), 354, **2016**.
3.  ZHANG, Y., LI T.T., SHIU B.C., SUN F., REN H.T., ZHANG X., LOU C.W., LIN J.H. Eco-friendly versatile protective polyurethane/triclosan coated polylactic acid nonwovens for medical covers application. Journal of Cleaner Production, **282**, 124455, **2021**.
4.  ZIA F., ZIA K.M., NAZIL Z.I., TABASUM S., KHOSA M.K., ZUBER M., Preparation of hydroxyethyl cellulose/ halloysite nanotubes graft polylactic acid-based polyurethane bionanocomposites. International Journal of Biological Macromolecules, **153**, 591, **2020**.
5.  ZHAO X., SHOU T., LIANG R., HU S., YU P., ZHANG L. Bio-based thermoplastic polyurethane derived from polylactic acid with high-damping performance. Industrial Crops and Products, **154**, 112619, **2020**.
6.  AN X., MA H., LIU B., WANG J. Graphene oxide reinforced polylactic acid/polyurethane antibacterial composites. Journal of Nanomaterials, **2013**, 373414, **2013**.
7.  NOREEN A., ZIA K.M., TABASUM S., AFTAB W., SHAHID M., ZUBER M. Hydroxyethylcellulose-g-poly(lactic acid) blended polyurethanes: Preparation, characterization and biological studies. International Journal of Biological Macromolecules, **151**, 993, **2020**.
8.  JAŠO V., GLENN G., KLAMCZYNSKI A., PETROVIĆ Z.S. Biodegradability study of polylactic acid/ thermoplastic polyurethane blends. Polymer Testing, **47**, 1, **2015**.
9.  DOGAN S.K., BOYACIOGLU S., KODAL M., GOKCE O., OZKOC G. Thermally induced shape memory behavior, enzymatic degradation and biocompatibility of PLA/TPU blends: "Effects of compatibilization". Journal of the Mechanical Behavior of Biomedical Materials, **71**, 349, **2017**.
10. LV S., ZHANG Y., TAN H. Thermal and thermo-oxidative degradation kinetics and characteristics of poly (lactic acid) and its composites. Waste Management, **87**, 335, **2019**.
11. KAMENO N., YAMADA S., AMIMOTO T., AMIMOTO K., IKEDA H., KOGA N. Thermal degradation of poly(lactic acid) oligomer: Reaction mechanism and multistep kinetic behavior. Polymer Degradation and Stability, **134**, 284, **2016**.
12. WANG Y., RUAN C., SUN J., ZHANG M., WU Y., PENG K. Degradation studies on segmented polyurethanes prepared with poly (d, l-lactic acid) diol, hexamethylene diisocyanate and different chain extenders. Polymer Degradation and Stability, **96**(9), 1687, **2011**.
13. OTHMAN M.B.H., KHAN A., AHMAD Z., ZAKARIA M.R., ULLAH F., AKIL H.M. Kinetic investigation and lifetime prediction of Cs–NIPAM–MBA-based thermo-responsive hydrogels. Carbohydrate Polymers, **136**, 1182, **2016**.
14. VVAZOVKIN S., BURNHAM A.K., CRIADO J.M., PÉREZ-MAQUEDA L.A., POPESCU C., SBIRRAZZUOLI N. ICTAC Kinetics Committee recommendations for performing kinetic computations on thermal analysis data. Thermochimica Acta, **520** (1/2), 1, **2011**.
15. ABOULKAS A., El HARFI K., El BOUADILI A. Thermal degradation behaviors of polyethylene and polypropylene. Part I: Pyrolysis kinetics and mechanisms. Energy Conversion and Management, **51** (7), 1363, **2010**.
16. FENG Y., WANG B., WANG F., ZHAO Y., LIU C., CHEN J., SHEN C. Thermal degradation mechanism and kinetics of polycarbonate/silica nanocomposites. Polymer Degradation and Stability, **107**, 129, **2014**.

17. STANĆIN H., MIKULČIĆ H., MANIĆ N., STOJILJIKOVIĆ D., VUJANOVIĆ M., WANG X., DUIĆ N. Thermogravimetric and kinetic analysis of biomass and polyurethane foam mixtures Co-Pyrolysis. Energy, **237** (Dec.15 Pt.2), 121592, **2021**.

18. YAO F., WU Q., LEI Y., GUO W., XU Y. Thermal decomposition kinetics of natural fibers: Activation energy with dynamic thermogravimetric analysis. Polymer Degradation and Stability, **93** (1), 90, **2008**.

19. TROVATI G., SANCHES E.A., NETO S.C., MASCARENHAS Y.P., CHIERICE G.O. Characterization of polyurethane resins by FTIR, TGA, and XRD. Journal of Applied Polymer Science, **115** (1), 263, **2010**.

20. YANG R., WANG B., LI M., ZHANG X., LI J. Preparation, characterization and thermal degradation behavior of rigid polyurethane foam using a malic acid based polyols. Industrial Crops and Products, **136**, 121, **2019**.

21. ARSHAD M.A., MAAROUFI A.K. An innovative reaction model determination methodology in solid state kinetics based on variable activation energy. Thermochimica Acta, **585**, 25, **2014**.

22. CHEN W., QI C., LI Y., TAO H. The degradation investigation of biodegradable PLA/PBAT blend: Thermal stability, mechanical properties and PALS analysis. Radiation Physics and Chemistry, **180**, 109239, **2021**.

23. ZHAO J., PAN H., YANG H., BIAN J., ZHANG H., GAO G., DONG L. Study on miscibility, thermal properties, degradation behaviors, and toughening mechanism of poly(lactic acid)/poly (ethylene-butylacrylate-glycidyl methacrylate) blends. International Journal of Biological Macromolecules, **143**, 443, **2020**.

24. VOLLI V., GOLLAKOTA A.R.K., SHU C.M. Comparative studies on thermochemical behavior and kinetics of lignocellulosic biomass residues using TG-FTIR and Py-GC/MS. Science of The Total Environment, **792**, 148392, **2021**.

25. HUANG G., ZOU Y., XIAO M., WANG S., LOU W., HAN D., MENF Y. Thermal degradation of poly(lactide-co-propylene carbonate) measured by TG/FTIR and Py-GC/MS. Polymer Degradation and Stability, **117**, 16, **2015**.